



Article

# Vehicle Route Planning of Diverse Cargo Types in Urban Logistics Based on Enhanced Ant Colony Optimization

Lingling Tan <sup>\*</sup>, Kequan Zhu and Junkai Yi

School of Automation, Beijing Information Science and Technology University, Beijing 100192, China; zhukq@bistu.edu.cn (K.Z.); yijk@bistu.edu.cn (J.Y.)

\* Correspondence: tanlingling@bistu.edu.cn

**Abstract:** In the realm of urban logistics, optimizing vehicle routes for varied cargo types—including refrigerated, fragile, and standard cargo—poses significant challenges amid complex urban infrastructures and heterogeneous vehicle capacities. This research paper introduces a novel model for the multi-type capacitated vehicle routing problem (MT-CVRP) that harnesses an advanced ant colony optimization algorithm, dubbed Lévy-EGACO. This algorithm integrates Lévy flights and elitist guiding principles, enhancing search efficacy and pheromone update processes. The primary objective of this study is to minimize overall transportation costs while optimizing the efficiency of intricate route planning for vehicles with diverse load capacities. Through rigorous simulation experiments, we corroborated the validity of the proposed model and the effectiveness of the Lévy-EGACO algorithm in optimizing urban cargo transportation routes. Lévy-EGACO demonstrated a consistent reduction in transportation costs, ranging from 1.8% to 2.5% compared to other algorithms, across different test scenarios following base data modifications. These findings reveal that Lévy-EGACO substantially improves route optimization, presenting a robust solution to the challenges of MT-CVRP within urban logistics frameworks.

**Keywords:** vehicle routing problem; urban logistics; ant colony optimization; Lévy flights; cost minimization



**Citation:** Tan, L.; Zhu, K.; Yi, J. Vehicle Route Planning of Diverse Cargo Types in Urban Logistics Based on Enhanced Ant Colony Optimization. *World Electr. Veh. J.* **2024**, *15*, 405. <https://doi.org/10.3390/wevj15090405>

Academic Editors: Liguozang and Leilei Zhao

Received: 23 July 2024

Revised: 30 August 2024

Accepted: 2 September 2024

Published: 4 September 2024



**Copyright:** © 2024 by the authors. Published by MDPI on behalf of the World Electric Vehicle Association. Licensee MDPI, Basel, Switzerland. This article is an open access article distributed under the terms and conditions of the Creative Commons Attribution (CC BY) license (<https://creativecommons.org/licenses/by/4.0/>).

## 1. Introduction

### 1.1. The Vehicle Routing Problem and Its Derivatives

As urbanization accelerates and populations continue to grow, the logistics and transportation industry has become an indispensable part of modern society. Consequently, the vehicle routing problem (VRP) has gained significant importance. The VRP aims to optimize vehicle usage during delivery or service provision to minimize costs and maximize efficiency [1]. This problem is not only theoretically challenging but also widely applicable in practical scenarios, including urban delivery, courier services, and public transportation planning.

The VRP encompasses a variety of derivatives, each of which is tailored to address specific constraints and operational demands. For instance, the capacitated vehicle routing problem (CVRP) focuses on optimizing the number of vehicles and the total distance traveled in scenarios where each vehicle has a fixed carrying capacity. Other notable variants include the vehicle routing problem with time windows (VRPTW), where deliveries must be completed within specific timeframes, and the green vehicle routing problem (GVRP), which considers environmental impacts such as fuel consumption and CO<sub>2</sub> emissions. These variations of VRP illustrate the problem's adaptability and relevance across different logistical challenges.

Furthermore, urban logistics face the significant challenge of managing diverse cargo types with unique transportation needs. The effective movement of varied goods—from perishables and fragile items to general merchandise—is essential not only for sustaining

economic growth but also for enhancing the operational efficiency of urban systems. To address these complex demands, logistics operations often employ specialized solutions such as the multi-type capacitated vehicle routing problem (MT-CVRP), which specifically caters to the varied capacity needs of different goods.

Faced with such complex routing challenges, which involve multiple objectives, numerous constraints, and dynamic environments, various metaheuristic algorithms, such as simulated annealing (SA), genetic algorithms (GA), particle swarm optimization (PSO), and ant colony optimization (ACO), stand out due to their high flexibility [2,3]. These algorithms have been extensively applied and developed in the relevant fields of study, proving indispensable in navigating the complexities of VRP and its derivatives. This highlights the ongoing need for robust, adaptable solutions in the face of evolving logistical challenges.

### 1.2. Overview of Metaheuristic Algorithms

Metaheuristic algorithms represent a class of strategies used for solving optimization problems, particularly excelling in their adaptability and efficiency in handling complex or NP-hard challenges. Although these algorithms do not guarantee the discovery of an optimal solution, they can sufficiently deliver effective solutions within a reasonable timeframe. The design of metaheuristic algorithms often draws inspiration from natural phenomena, such as genetic algorithms that simulate biological evolution, ant colony optimization algorithms that mimic the behavior of ants optimizing their paths to food sources, and simulated annealing algorithms that are based on the annealing process in solid-state physics.

Among the wide array of metaheuristic algorithms employed, various methods, such as SA, GA, and PSO, have been extensively developed and applied in the field. For example, Sarbijan and Behnamian [4] introduced a hybrid particle swarm optimization-simulated annealing algorithm to tackle the multi-fleet feeder vehicle routing problem, demonstrating that the hybrid approach had provided significant improvements in terms of solution quality and efficiency over traditional methods, like ant colony optimization and variable neighborhood search, particularly in large-sized instances. Allsager et al. [5] introduced a novel hybrid approach combining cuckoo search (CS) with simulated annealing for solving the capacitated vehicle routing problem (CVRP). This method integrates twelve distinct neighborhood structures and a disruptive selection strategy, demonstrating significant improvements in solution quality. Holló-Szabó and Botzheim [6] addressed the asymmetric capacitated vehicle routing problem (ACVRP) using the bacterial memetic algorithm (BMA), which improved convergence and effectiveness by combining global and local search techniques. Yang and Tao [7] introduced a bi-objective optimization model in cold chain logistics, employing a hybrid simulated annealing non-dominated sorting genetic algorithm II (SA-NSGA-II) algorithm that effectively balances cost reduction and customer satisfaction, as demonstrated in their numerical experiments. Gu et al. [8] tackled the multi-depot vehicle routing problem (MDVRP) by initially simplifying it to a single-depot format through depot clustering. They employed an adapted artificial bee colony algorithm, which was enhanced by a coevolution strategy for depot combination; the test results demonstrated substantial improvements. Ahmed et al. [9] presented a genetic algorithm and four hybrid genetic algorithms tailored for the asymmetric distance-constrained vehicle routing problem (ADVRP). These methods incorporate 2-opt search and local search techniques to enhance solution quality. Their research involves comparative testing on the TSPLIB with multiple vehicles, indicating that hybrid genetic algorithms, particularly those incorporating local search, provide competitive performance in both restricted and unrestricted ADVRP scenarios. Li et al. [10] addressed the electric vehicle routing problem with time windows (EVRPTW) using an enhanced remove-reinsert genetic algorithm (RI-GA). This refined approach focuses on reducing energy consumption and transportation costs through a targeted removal and reinsertion strategy, achieving faster convergence and lower routing costs compared to traditional methods. Their results, validated in a real-world scenario

involving apple transportation in New York's Hudson Valley, underscore the practical benefits of RI-GA. Liu et al. [11] enhanced E-grocery distribution efficiency by optimizing a two-echelon vehicle routing problem with the integration of autonomous delivery vehicles (ADV). Utilizing a clustering-based hybrid genetic algorithm and particle swarm optimization (C-GA-PSO), the study efficiently managed routing from conventional vans to ADVs. The results show the algorithm's effectiveness at various customer scales and offer insights into how depot layout and customer density impact overall costs, aiding in the strategic planning of sustainable E-grocery delivery networks. Ji et al. [12] introduced a novel hybrid algorithm, adaptive cat swarm optimization (ACSO), which melds the strengths of cat swarm optimization (CSO) and adaptive particle swarm optimization (APSO). This algorithm optimizes search capabilities through enhanced strategies, such as a controlled tracing radius and an adaptive random number parameter. Zacharia et al. [13] tackled the vehicle routing problem with fuzzy payloads, aiming to minimize both travel distance and fuel consumption using a bi-objective genetic algorithm. This approach incorporates fuzziness, addressing uncertainties in payload quantities, and enhances routing efficiency in real-world scenarios. Li et al. [14] developed a novel concentration-immune algorithm particle swarm optimization (C-IAPSO), blending the strengths of concentration-immune algorithm (C-IA) and PSO for vehicle path optimization in intelligent logistics systems. Tested against standard functions, C-IAPSO demonstrates superior convergence speeds and marked improvements in accuracy for specific functions, such as sphere and quadric. When applied to urban rail-based logistics distribution, C-IAPSO optimized the routing, illustrating significant enhancements in transportation efficiency and cost reduction.

In addition to the aforementioned metaheuristic algorithms and their variants, which have shown substantial benefits in solving various complex vehicle routing problems, another powerful approach warrants particular attention. ACO, well suited for VRP types of issues, will be explored in greater detail in the following section. This will include a detailed discussion of its technical aspects and practical applications.

### 1.3. Applications of ACO

Among the plethora of optimization algorithms, ACO is widely employed due to its efficient search capabilities and outstanding distributed computing characteristics. This algorithm has been theoretically proven to be applicable to a wide range of optimization challenges [15,16], including complex problems such as route planning [17], resource scheduling [18,19], and network design [20]. Compared to other metaheuristic algorithms, ACO possesses distinct advantages, such as a robust positive feedback mechanism that facilitates rapid convergence to high-quality solutions, exceptional distributed computing capabilities suitable for large-scale problems, and high flexibility and robustness in dynamic environments.

For example, Lesch et al. [21] developed a two-stage strategy with a timeline algorithm for handling time windows and pause times, using GA and ACO to address real-world constraints in VRP, showing that their method outperforms four state-of-the-art algorithms in managing these constraints efficiently. Huang et al. [22] explored the integration of drones with trucks in parcel delivery within the vehicle routing problem with drone (VRPD) by ACO. Their approach not only minimizes costs and CO<sub>2</sub> emissions but also proves more efficient in reducing delivery times compared to traditional vehicle routing methods, with substantial cost savings of over 30% for large instances. Frías et al. [23] presented four hybrid algorithms addressing the energy minimizing vehicle routing Problem (EMVRP), combining machine learning clustering and ACO techniques. These algorithms were tested using CVRPLIB instances, showing efficient solutions and promising results that call for further experimentation and tuning. Furthermore, the ongoing in-depth research by numerous scholars has led to the increasingly mature and widespread technical applications of ACO [24].

Compared with other heuristic algorithms, the positive feedback mechanism in the ant colony algorithm makes ants tend to choose paths with higher pheromone concentrations

during the search process, and this choice further increases the pheromones on these paths, thus attracting more ants. This mechanism helps the algorithm to converge quickly, but at the same time, it may cause the algorithm to prematurely focus on some paths, ignoring other potentially better paths, and fall into local optimal solutions. Many computing tasks in the ACO algorithm can be parallelized, such as the calculation and updating of pheromones, which can be distributed on multiple cores of the CPU at the same time, reducing the computation time.

Although the ACO algorithm has demonstrated robust performance in addressing VRP types of challenges, enhancing its exploratory capabilities and preventing stagnation at local optima remain critical areas for improvement. To address these issues, we need to further improve the ACO algorithm. The current study integrates Lévy flight into the ACO framework, which is a strategy inspired by random, scale-free natural movements. This integration capitalizes on Lévy flight's ability to facilitate extensive movements within the solution space, thereby significantly enhancing the algorithm's potential for thorough exploration and optimization.

#### 1.4. Lévy Flight

Lévy flight, named after the French mathematician Paul Lévy, refers to a class of random walks in which step lengths are governed by Lévy distributions. This statistical pattern allows for occasional long jumps, significantly enhancing the search process over large solution spaces and providing a powerful mechanism to escape from local optima. The 'heavy-tailed' nature of Lévy distributions is crucial to their functionality; it ensures that the probability of taking very long steps does not decay as quickly as that in normal distributions, enabling the search to span wider areas more effectively. Such capabilities make Lévy flights particularly useful for global optimization challenges encountered in complex problem domains.

Given these unique properties, Lévy flights have been widely adopted to improve the efficacy of various metaheuristic algorithms. Their ability to facilitate extensive searches and prevent premature convergence is highly valued in scenarios where traditional algorithms struggle. For example, Li et al. [25] explored the integration of Lévy flight in metaheuristic algorithms, such as cuckoo, monarch butterfly optimization, and moth search algorithms, enhancing their ability to escape local optima. Their study covers statistical analysis, classification of uses, and future research directions of Lévy flight. Shen et al. [26] addressed the multi-compartment electric vehicle routing problem with soft time windows and multiple charging types (MCEVRP-STW and MCT), utilizing a Lévy flight-based estimation distribution algorithm (EDA-LF) for optimization. These studies collectively demonstrate the effective role of Lévy flights in advancing the fields of optimization and path planning. Through innovative algorithmic integrations and applications, Lévy flights contribute significantly to enhancing solution quality and efficiency in complex scenarios.

In summary, this paper models the vehicle routing problem for various types of urban cargo and proposes an enhanced ant colony optimization algorithm, Lévy-EGACO, which integrates Lévy flights and elitist guiding strategies. Section 2 will present the constraint conditions and symbol definitions of the model under study. Section 3 will elaborate on the design of the entire algorithmic process. Section 4 will conduct simulations and display the resulting data. The final section, Section 5, will summarize the findings of the paper. This work provides new insights and methods for applying ant colony algorithms in complex model optimization domains.

## 2. Problem Description and Modeling

According to the literature, modern logistics networks can be categorized into global, regional, and urban levels. The distribution path of a piece of goods requires a hierarchical path planning method. This model is developed based on the common constraints and challenges of path planning across all logistics levels.

In the context of urban logistics, MT-CVRP can be described as the challenge of managing the transportation of various types of goods across a logistics center’s service area. Given the known quantities of different goods at each distribution point, various types of delivery vehicles must depart from the logistics center, traverse the area, and deliver the required goods to all designated sites. In the case of meeting the delivery time, the objective is to minimize the total costs, which include both operational and routing expenses, such as costs for vehicles, personnel, fuel, environmental protection, etc.

The specific constraints are as follows:

- Each vehicle departs from and returns to a single logistics center, with an ample supply of each type of vehicle available;
- Each distribution site is serviced once by the corresponding type of delivery vehicle;
- Each type of vehicle is only capable of transporting specific types of cargo in order to enhance the quality of transportation and ensure customer satisfaction;
- Vehicle movement between sites is unidirectional, and vehicles cannot backtrack;
- Vehicles are not permitted to alter their route mid-journey and must follow the pre-determined path;
- Vehicles are considered to be unloaded when they leave the logistics center for the first distribution site, and the load must not exceed the maximum capacity defined for that vehicle type during transportation.

The parameter settings are shown in Table 1.

**Table 1.** Parameter settings.

Symbols	Definitions
$O = \{1, 2, 3, \dots, o, o+1\}$	The set of site includes $o$ distribution sites, with the logistics center designated as site $o+1$ .
$V = \{1, 2, 3, \dots, j\}$	The set of vehicle numbers consists of $j$ vehicles.
$T = \{1, 2, 3, \dots, h\}$	The set of cargo types includes $h$ different types of goods.
$W = \{1, 2, 3, \dots, n\}$	The set of vehicle types comprises $n$ models.
$cap_w$	The maximum load capacity of vehicle type $w$ .
$c_w$	The unit transportation cost per distance for vehicle type $w$ .
$s_w$	The startup cost for vehicle type $w$ .
$d_t$	The maximum allowable transport distance of cargo type $t$ .
$q_{il}$	The quantity of cargo type $l$ at distribution site $i$ .
$a, b \in O$	Transportation route nodes $a$ and $b$ .
$d_{ab}$	The distance between nodes $a$ and $b$ .
$e_{ab}$	The traffic congestion coefficient between nodes $a$ and $b$ , $e_{ab} \geq 1$ .
$g_{vw} \in \{0,1\}$	If vehicle $v$ belongs to vehicle type $w$ , then $g_{vw} = 1$ , otherwise 0.
$h_{wt} \in \{0,1\}$	If vehicle type $w$ transports cargo type $t$ , then $h_{wt} = 1$ , otherwise 0.
$m_{wt} \in \{0,1\}$	If vehicle type $w$ can transport cargo type $t$ , then $m_{wt} = 1$ , otherwise 0.
$x_v \in \{0,1\}$	If vehicle $v$ is activated, then $x_v = 1$ , otherwise 0.
$y_{abv} \in \{0,1\}$	If vehicle $v$ transports from node $a$ to node $b$ , then $y_{abv} = 1$ , otherwise 0.
$C$	The total cost, including startup and transportation costs.

Based on the specified parameters and constraints, the following mathematical model can be established:

$$minC = \sum_{v=1}^j \sum_{w=1}^n g_{vw} s_w x_v + \sum_{a=1}^{o+1} \sum_{b=1}^{o+1} \sum_{v=1}^j \sum_{w=1}^n c_w g_{vw} e_{ab} d_{ab} y_{abv} \tag{1}$$

Equation (1) defines the objective function, representing the total cost.

$$\sum_{a=1}^{o+1} \sum_{v=1}^j y_{aiv} g_{vw} = 1, \forall i \in O \setminus \{o+1\}, \forall w \in W \tag{2}$$

$$\sum_{b=1}^{o+1} \sum_{v=1}^j y_{ibv} g_{vw} = 1, \forall i \in O \setminus \{o+1\}, \forall w \in W \quad (3)$$

Equations (2) and (3) stipulate that only a single vehicle of type  $w$  may visit site  $i$ .

$$\sum_{a=1}^{o+1} y_{aiv} \leq x_v, \forall i \in O \setminus \{o+1\}, \forall v \in V \quad (4)$$

Equation (4) ensures that vehicle  $v$  services site  $i$  only once.

$$\sum_{i=1}^o y_{(o+1)iv} = \sum_{i=1}^o y_{i(o+1)v} = x_v, \forall v \in V \quad (5)$$

Equation (5) requires that vehicle  $v$  must start from the logistics center, complete its delivery tasks, and then return.

$$y_{aiv} + y_{iav} \leq 1, \forall i, a \in O \setminus \{o+1\}, \forall v \in V \quad (6)$$

Equation (6) dictates that vehicle  $v$  can only travel in one direction between sites.

$$h_{wt} \leq m_{wt}, \forall w \in W, \forall t \in T \quad (7)$$

Equation (7) ensures that model  $w$  can only be loaded with the type of cargo  $h$  that is permitted to be transported.

$$\sum_{a=1}^{o+1} \sum_{i=1}^{o+1} g_{vw} h_{wt} e_{ai} d_{ai} y_{aiv} \leq d_t, \forall v \in V, \forall w \in W, \forall t \in T \quad (8)$$

Equation (8) ensures that the transportation distance for each item of cargo is within the maximum allowable limit and verifies that the transportation time for cargoes meets user requirements.

$$\sum_{a=1}^{m+1} \sum_{i=1}^m \sum_{t=1}^h q_{it} g_{vw} h_{wt} y_{aiv} \leq g_{vw} cap_w, \forall v \in V, \forall w \in W \quad (9)$$

Equation (9) sets the maximum load capacity for vehicle  $v$ .

$$y_{abv} \leq x_v, \forall a, b \in O, \forall v \in V \quad (10)$$

Equation (10) addresses the startup constraints for vehicle  $v$ .

$$x_v \in \{0, 1\}, \forall v \in V \quad (11)$$

$$y_{abv} \in \{0, 1\}, \forall a, b \in O, \forall v \in V \quad (12)$$

Equations (11) and (12) are binary constraints.

### 3. Enhanced Ant Colony Algorithm Design

The ACO algorithm is a heuristic approach that simulates the foraging behavior of ants to solve combinatorial optimization problems. In nature, ants release pheromones during their search for food, and other ants choose their paths based on the concentration of these pheromones. Given the complex requirements of the MT-CVRP, traditional ACO requires design enhancements. By integrating Lévy flights and elitist guiding strategies, the enhanced ant colony algorithm, Lévy-EGACO, is able to escape local optima more effectively, thereby improving the efficiency and accuracy of solutions. The specific steps to solve the problem are as follows.



### 3.1. Information Gathering

Based on the problem description, the known information includes the following:

- The distance matrix between various sites and the logistics center;
- The quantities of various types of goods at each site, measured in tons;
- The types of goods that can be transported by each vehicle type, along with their maximum load capacities;
- The activation and distance costs for each vehicle model.

Given that there are currently  $o$  distribution sites, and the logistics center is designated as site  $o+1$ , then an initial pheromone matrix of size  $(o+1) \cdot (o+1)$  can be generated as follows:

$$\begin{bmatrix} 0 & \tau_0 & \tau_0 & \cdots & \tau_0 \\ \tau_0 & 0 & \tau_0 & \cdots & \tau_0 \\ \tau_0 & \tau_0 & 0 & \cdots & \tau_0 \\ \vdots & \vdots & \vdots & \ddots & \vdots \\ \tau_0 & \tau_0 & \tau_0 & \cdots & 0 \end{bmatrix} \quad (13)$$

where  $\tau_0$  represents the initial pheromone value, and the pheromone values at diagonal positions are typically set to 0.

### 3.2. Create Paths

Define the number of ants as  $N$ , and place them at the logistics center. The path traversed by each ant is considered as the collection of routes for all vehicles of a certain type. Take ant  $k$  as an example. When it is at the logistics center and has not yet departed, its load is zero, and its path is defined as  $Path = [o+1]$ . At this point, it evaluates all sites based on its maximum load capacity,  $cap_w$ , to generate a list of feasible sites that will not cause it to be overloaded. The list of feasible sites for ant  $k$ , starting from the logistics center with zero load, should be  $[1, 2, 3, \dots, o]$ .

After obtaining the list of feasible sites, the ant uses a roulette wheel selection rule to independently choose the next site to visit, with probability  $p_{ij}^k$ . The calculation of probability  $p_{ij}^k$  is as follows:

$$p_{ij}^k = \frac{[\tau_{ij}(t)]^\alpha [\eta_{ij}]^\beta}{\sum_{j \in Allowed_k} [\tau_{ij}(t)]^\alpha [\eta_{ij}]^\beta} \quad (14)$$

Herein,  $\tau_{ij}(t)$  denotes the pheromone intensity from site  $i$  to site  $j$  at time  $t$ ; that is, during the  $t$ -th iteration;  $\eta_{ij}$  represents the heuristic factor from site  $i$  to site  $j$ , defined as the reciprocal of the distance between site  $i$  to site  $j$ .  $Allowed_k$  denotes the list of feasible sites for ant  $k$ , and  $\alpha$  and  $\beta$  are parameters that control the importance of the pheromone strength and the heuristic factor, respectively.

If ant  $k$  selects site 3 as its next destination, its path can be considered as  $Path = [o+1, 3]$ , with a load size of  $cap_3$ . At this point, it will continue to assess all remaining sites and generate a new list of feasible sites. After multiple selections and departures, as the load approaches its limit and no more eligible sites are available for selection,  $k$  will return to the logistics center.

Assume its path is  $Path = [o+1, 3, 2, o+1]$ , and upon returning to the logistics center, it unloads and departs again. Upon restarting, the list of feasible sites also removes sites 3 and 2. After repeatedly departing from and returning to the logistics center, it generates a path as  $Path = [o+1, 3, 2, o+1, 6, 4, 5, o+1, \dots, 8, o+1]$ . Each cycle of departure from and return to the logistics center is isolated and considered as the route planning for all vehicles of a specific type. From this process, the required number of vehicles, each vehicle's route, and the current cost  $C$  can be calculated using Equation (15):

$$C = C_{path} + C_{vehicle} \quad (15)$$

Herein,  $C_{path}$  represents the transportation cost associated with the route, and  $C_{vehicle}$  denotes the vehicle activation cost. Following the steps outlined above, the path creation for ant  $k$  is completed, and the next ant begins to construct its path.

### 3.3. Cost Optimization

Since ants return to the logistics center only when nearly fully loaded, introducing an additional vehicle while allowing the remaining vehicles to return earlier might reduce transportation distances and lower overall costs.

Based on this idea, by appending the logistics center site at the end of the route and transferring sites, the algorithm can search for potentially cost-reducing paths. The practical steps are as follows:

- In the existing route  $Path$ , add a new logistics center site  $o+1$  at the end of the path. Taking site 6 as the transfer site, execute the relocation of cargo sites, and recalculate costs accordingly, as shown in Figure 1.
- Perform a relocation operation for each site  $i$ . It is possible to recalculate the new load  $C_{i-new}$  and the cost changes associated with the transportation route  $C_{i-path}$ .
- If  $cap_{i-new} < cap_w$ , select the minimum value among  $C_{i-path}$  values, denoted as  $C_{i-path-min}$ . If  $C_{path} - C_{i-path-min} > 0$ , it indicates that relocating site  $i$  has reduced the path costs. Return to step 2 to continue new relocation operations, eventually generating  $Path_{new}$ , and proceed to step 4. Otherwise, continue with  $Path_{new} = Path$ , and move to step 5.
- Utilize  $Path_{new}$ , the pathway modified following site translocations, as the prevailing route. Employ Equation (15) to calculate the revised aggregate costs,  $C_{new}$ . And if the calculation results in  $C - C_{new} < 0$ , this indicates that the strategic addition and relocation of sites within the new configuration have effectively reduced the total costs. Subsequently, redefine  $Path$  as  $Path_{new}$ , and revert to step 1 for additional site relocation activities. Conversely, if  $C - C_{new} > 0$ , indicating that the integration of additional vehicles has not yielded a cost reduction, persist with the initial route configuration, setting  $Path_{new} = Path$ .
- Output the optimized path with reduced costs.

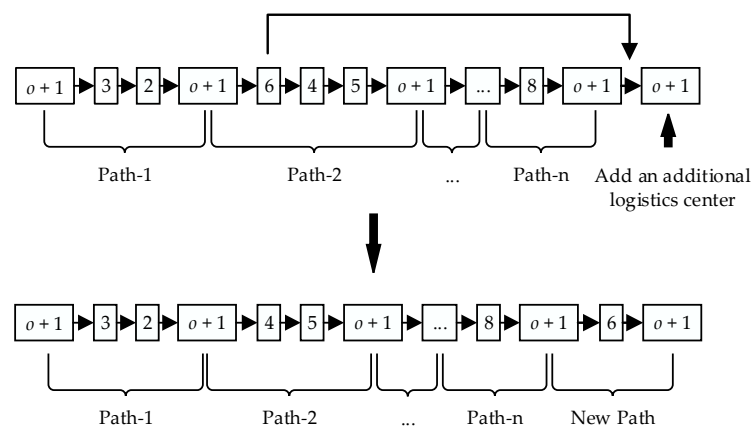


Figure 1. Vehicle addition and site relocation.

### 3.4. Pheromone Update

Once the optimal  $Path$  from ant  $k_{best}$  is determined, it is first compared with the currently known best cost path,  $Path_{best}$ . If the cost  $C_{best}$  of  $Path_{best}$  is greater than the cost  $C$  of the current path, then  $Path_{best}$  is updated to  $Path$ ; if it is the first iteration, then directly set  $Path_{best} = Path$ . Following this update, based on the cost-optimal  $Path_{best}$ , the pheromone levels across the entire distance matrix are updated. This update includes processes for pheromone reinforcement and pheromone evaporation, which are essential for guiding the subsequent search efforts of the ants.



As demonstrated in Equation (16), pheromone intensification implies that ants deposit pheromones based on the cost of the path they have discovered:

$$\Delta\tau_{ij}^k = \frac{1}{\eta C^k} \tag{16}$$

where  $C^k$  is the cost associated with  $Path_{best}^k$ , and  $\eta$  is a proportional constant.

Pheromone evaporation, as depicted in Equation (17), occurs along each edge where pheromones evaporate at a specified rate:

$$\tau_{ij}(t+1) = (1 - \rho)\tau_{ij}(t) \tag{17}$$

where  $\rho$  is the evaporation coefficient. Consequently, the method for pheromone updating can be derived by combining Equations (16) and (17), as shown in Equation (18):

$$\tau_{ij}(t+1) = (1 - \rho)\tau_{ij}(t) + \sum_k \Delta\tau_{ij}^k \tag{18}$$

### 3.5. Lévy Flights and Elitist Guiding

During deeper iterations of the ant colony algorithm, it often encounters the issue of converging to local optima, which impedes further improvement in the quality of solutions. To overcome this challenge, the Lévy-EGACO algorithm employs a random restart strategy, involving reinitialization of the pheromone matrix. At this point, Lévy flights are utilized as an innovative method to generate a step-length matrix. After limiting the maximum step length and completing normalization, this matrix can serve as the initial values for each element in the pheromone matrix, thereby enhancing the exploratory and diversity aspects of the algorithm. This is combined with an elitist guiding strategy, which intensifies the pheromone concentration along the currently optimal paths.

As illustrated in Figure 2, Lévy flight's combination of short and long steps is congruent with the realities of various natural systems, such as the foraging and flight patterns of animals. It is commonly employed to manage fluctuations in economic data and signal processing, particularly in scenarios that necessitate rapid jumps across the search space. In practical applications, the Mantegna algorithm is commonly used to simulate Lévy flights, with the calculation method for the step length as follows:

$$L = \frac{\mu}{|v|^{\frac{1}{\beta}}} \tag{19}$$

where  $\mu$  and  $v$  are two normally distributed random variables, with  $\mu \sim N(0, \sigma_\mu^2)$ , and  $v \sim N(0, 1)$ . The  $\beta$  is the exponent parameter of the Lévy flight. The calculation method for  $\sigma_\mu^2$  is as follows:

$$\sigma_\mu = \left\{ \frac{\Gamma(1 + \beta)\sin\left(\frac{\pi\beta}{2}\right)}{\Gamma\left(\frac{1+\beta}{2}\right)\beta 2^{\frac{(\beta-1)}{2}}}\right\}^{\frac{1}{\beta}} \tag{20}$$

where  $\Gamma$  denotes the gamma function, and the variable  $\beta$  is typically set to 1.5.

$$\begin{bmatrix} 0 & \tau_{Lvy} & N_0\tau_{Lvy} & \cdots & \tau_{Lvy} \\ \tau_{Lvy} & 0 & \tau_{Lvy} & \cdots & N_0\tau_{Lvy} \\ \tau_{Lvy} & N_0\tau_{Lvy} & 0 & \cdots & \tau_{Lvy} \\ \vdots & \vdots & \vdots & \ddots & \vdots \\ N_0\tau_{Lvy} & \tau_{Lvy} & \tau_{Lvy} & \cdots & 0 \end{bmatrix} \tag{21}$$

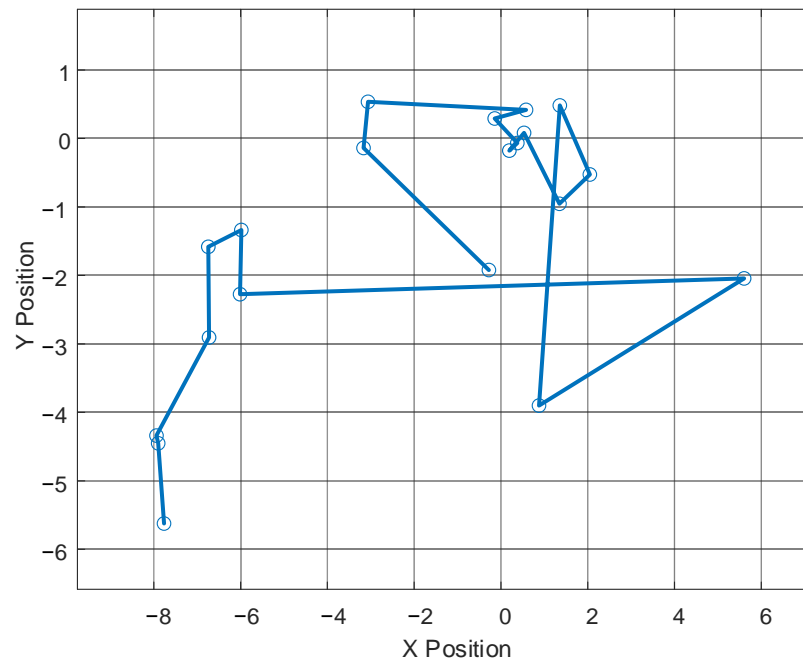


Figure 2. Lévy flight trajectory image.

The pheromone matrix following the implementation of the elitist guidance strategy is illustrated in Equation (21). Here,  $\tau_{Lévy}$  represents the pheromones generated through Lévy flights, and  $N_0$  is the intensification multiplier. After the creation of the Lévy flight matrix, the elitist guidance strategy is applied in conjunction with the historically optimal paths. The core idea of this strategy is to enhance the pheromone concentration on portions of known good solutions, thereby making subsequent ants more inclined to choose these routes. The complete flowchart for the Lévy flight and elitist guidance segment is shown in Figure 3.

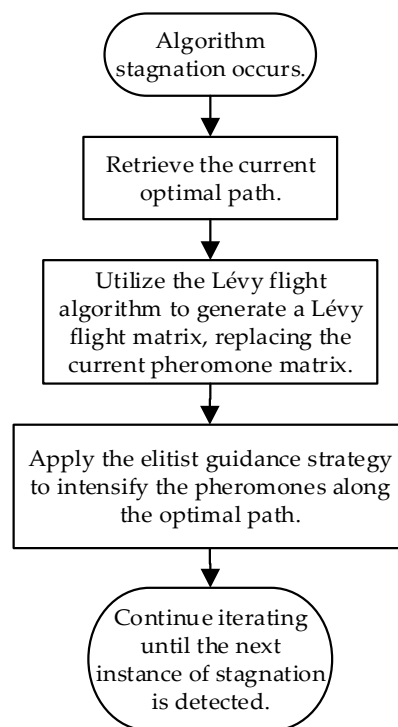


Figure 3. Lévy flight and elitist guidance process.

Elitist guidance in optimization algorithms is conceptually akin to the notion of velocity in PSO, as both are instrumental in directing the search within the solution space toward previously identified optimal solutions. However, a significant difference exists in their mechanisms of action, which means elitist guidance is primarily utilized during random restarts and does not exert a continuous influence across iterations. This specific application helps to prevent the algorithm from prematurely converging on local optima, thereby encouraging a more comprehensive exploration of the solution space. In this refined approach, the integration of Lévy flights with random restarts and elitist guidance achieves a harmonious balance between maintaining diversity in the solution pool and enabling deep exploration of the algorithmic landscape. When the iteration limit is reached, the algorithm identifies and outputs the historically optimal solution. This solution not only specifies the optimal paths but also outlines the overall lowest costs associated with each vehicle type, effectively optimizing logistical efficiencies in complex transportation networks.

## 4. Simulation

### 4.1. Simulation Construction

In line with established urban transportation paradigms, this study differentiates among three distinct vehicle types tailored for specific cargo needs: refrigerated cargo trucks, fragile cargo trucks, and standard cargo trucks. These vehicles are respectively earmarked for transporting perishable goods, fragile items, and general cargo, with respective maximum load capacities set at 5 tons, 2 tons, and 4.5 tons. The transportation cost per kilometer is delineated at USD 4, USD 3.5, and USD 3 for each vehicle type, while daily startup costs for long-term rentals are determined to be USD 10, USD 8, and USD 6 per vehicle, accordingly. Considering the environmental impact of the transportation process, the transportation cost per kilometer includes not only the fuel price but also the carbon emission fee. Daily startup costs include vehicle purchase or lease costs, transportation insurance costs, driver salaries, etc. Each vehicle class is stringently utilized for its designated cargo type, ensuring that transit conditions are meticulously optimized for the specific needs of each cargo category.

The simulation setting is orchestrated around a logistics hub situated in the Chaoyang District of Beijing, incorporating nine distribution nodes and one central logistics facility, sequentially numbered from one to ten. The intricacy of urban transportation infrastructure, featuring one-way streets, subterranean passages, and elevated roadways, engenders discrepancies in the bidirectional travel distances between these locations. This phenomenon bears a resemblance to the distance asymmetries characteristic of the asymmetric traveling salesman problem (ATSP), in which the travel expenditure from one point to another may differ from the cost in the opposing direction [27].

The geographical positions of these sites are depicted in Figure 4. The shortest driving distances between these sites have been measured using an open platform and are utilized as simulation data, with specific values presented in Table 2, expressed in kilometers. According to the real-time traffic congestion situation provided by the open platform, the traffic congestion coefficient  $e_{ab}$  will be updated every time, and the  $e_{ab}$  is equal to 1 when the traffic is unimpeded, the  $e_{ab}$  is equal to 1.5 when the traffic is normal congested, and the  $e_{ab}$  is equal to 2 when the traffic is very congested. Additionally, to simulate real-world scenarios and address the entire problem, the quantities of different types of cargo at each distribution site have been established, as shown in Table 3, measured in tons per day.

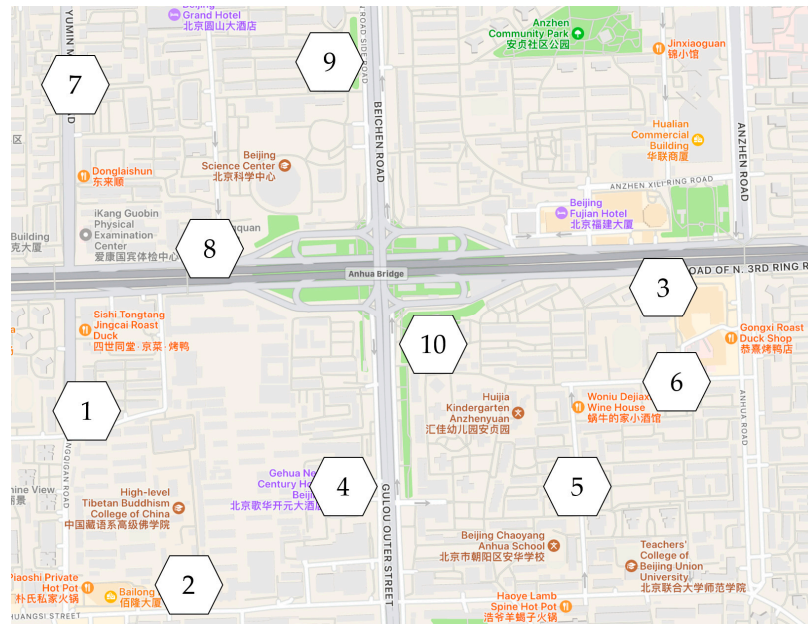


Figure 4. Schematic diagram of distribution sites.

Table 2. Round-trip distances between distribution sites.

Number	1	2	3	4	5	6	7	8	9	10
1	-	0.5	1.3	1.2	1.5	1.9	2.4	3.3	2.7	2.2
2	0.5	-	1.4	0.6	0.9	1.2	2.3	3.1	2.5	1.0
3	2.2	1.7	-	1.8	1.2	0.4	3.2	4.0	3.4	0.9
4	1.1	0.6	1.5	-	1.0	1.7	2.4	3.2	2.7	1.1
5	1.3	0.9	0.7	0.9	-	0.5	2.3	3.1	2.6	0.5
6	1.7	1.2	0.2	1.6	1.0	-	2.3	3.1	2.6	0.4
7	2.7	2.2	2.1	1.6	2.3	2.3	-	0.8	0.8	2.6
8	2.8	2.8	2.7	2.2	2.9	2.9	0.6	-	1.4	2.9
9	1.8	1.3	1.2	0.8	1.5	1.5	1.1	0.5	-	1.5
10	3.0	2.0	0.7	2.1	1.4	0.4	1.9	1.6	2.3	-

Table 3. Quantities of goods by type at each distribution site.

Number	Perishable Cargo	Fragile Cargo	Standard Cargo
1	2.13	0.49	2.68
2	2.31	0.16	1.78
3	0.75	0.49	1.59
4	2.33	0.48	1.22
5	1.76	0.29	2.71
6	0.70	0.42	1.76
7	1.06	0.16	1.61
8	1.59	0.27	2.65
9	2.42	0.47	1.65

#### 4.2. Simulation Results

To highlight the advantages of Lévy-EGACO, simulation experiments were conducted using the standard ACO and the adaptive genetic algorithm (AGA) for comparative purposes. The standard ACO employs a simpler pheromone update rule without the Lévy flights' heavy-tailed property and lacks the intervention of an elitist guidance strategy. The parameters for the standard ACO algorithm include the number of ants  $N$ , pheromone factor  $\alpha$ , heuristic information factor  $\beta$ , evaporation coefficient  $\rho$ , and the number of iterations

$N_{iter}$ . Lévy-EGACO additionally includes the elitist guidance intensification multiplier  $N_0$ ; and the random restart threshold  $\theta$ . Similarly, the AGA provides a basis for comparison by utilizing adaptive mechanisms for crossover and mutation rates, allowing for dynamic adjustment during the optimization process. The parameters for the AGA include the population size  $N$ , crossover rate  $p_c$ , mutation rate  $p_m$ , and adaptation factors for crossover and mutation rates  $\gamma_c$  and  $\gamma_m$ .

The simulation parameters are detailed in Table 4.

**Table 4.** Parameters.

Symbol			Definition	Value
AGA	ACO	Lévy-EGACO		
-	$\alpha$	$\alpha$	Pheromone factor	[0.5,2], step 0.1
-	$\beta$	$\beta$	Heuristic information factor	[1,3], step 0.1
-	$\rho$	$\rho$	Evaporation coefficient	[0.1,0.5], step 0.1
-	-	$N_0$	Elitist guidance intensification multiplier	2
-	-	$\theta$	Random restart threshold	20
$p_c$	-	-	Crossover rate	0.9
$p_m$	-	-	Mutation rate	0.1
$\gamma_c$	-	-	Adaptation factor for crossover rate	0.1
$\gamma_m$	-	-	Adaptation factor for mutation rate	0.1
$N_{iter}$	$N_{iter}$	$N_{iter}$	Number of iterations	500
$N$	$N$	$N$	Number of population size/ants	100/20

The standard ACO, Lévy-EGACO, and AGA algorithms will use relatively optimal parameter values to ensure the best possible results.

The number of ants  $N$  is set to 20, based on experimental results. A smaller group of ants might not adequately explore the complex search space, while a larger number could lead to wastage of computational resources and increased algorithm runtime; thus, 20 has been demonstrated to be the optimal balance between efficiency and effectiveness. Given the smaller scale model used in experiments and the lower computational complexity,  $\alpha$ ,  $\beta$ , and  $\rho$  can be determined within a predefined range through grid search.  $N_0$  is set to 2 to enhance the pheromone on high-quality paths, thereby making the algorithm more likely to revisit known quality paths. This value was determined based on observations of path stability and solution quality from multiple experiments.  $\theta$  is set to 20, based on the algorithm's performance once a local optimum is reached. When the algorithm fails to improve the current solution after 20 consecutive iterations, introducing a random restart helps to escape local optima and increases solution diversity.  $N_{iter}$  is set to 500, based on the average number of iterations needed for the algorithm to converge on similar problems. This value ensures sufficient time for the algorithm to conduct a thorough search within the solution space while also effectively managing the runtime of the algorithm. The initial crossover rate  $p_c$  and mutation rate  $p_m$  in the AGA algorithm are set to some classical values and can adaptively change during iterations based on the adaptation factors. Since the population size  $N$  in the AGA algorithm significantly impacts the algorithm's performance, setting a small population size may cause the algorithm to fall into local optima easily. Therefore, the population size is reasonably set to 100 as an initial value.

The hardware configuration used for the simulation consists of a standard personal computer platform running the Windows 10 operating system, equipped with an Intel Core i5-8300H processor. The programs were developed and executed using MATLAB R2022b. Following 20 runs of the algorithm, the average path costs for each type of cargo under both algorithms were calculated. The data obtained are presented in Table 5. The optimal paths and loads for each type of cargo obtained by the algorithm are shown in Table 6.

Table 5. Cost data results.

Cost	Lévy-EGACO			ACO			AGA		
	Best	Average	Optimal Ratio	Best	Average	Optimal Ratio	Best	Average	Optimal Ratio
Refrigerated	100.8	100.88	95%	102	103.14	45%	102	103.12	55%
Fragile	49.25	49.25	100%	49.25	49.25	100%	49.25	49.25	100%
Standard	186	186	100%	186	189.85	15%	186	190.05	10%
Total	336.05	336.13	-	337.25	342.24	-	337.25	342.42	-

Table 6. Transportation routes for each vehicle type.

Number	Vehicle Type	Transportation Route	Load/Ton
1	Refrigerated cargo trucks	10-6-1-5-10	4.59
2	Refrigerated cargo trucks	10-8-7-4-10	4.95
3	Refrigerated cargo trucks	10-9-2-10	4.73
4	Refrigerated cargo trucks	10-3-10	0.75
5	Fragile cargo trucks	10-6-3-5-1-2-10	1.85
6	Fragile cargo trucks	10-8-7-9-4-10	1.38
7	Standard cargo trucks	10-6-5-10	4.47
8	Standard cargo trucks	10-1-2-10	4.46
9	Standard cargo trucks	10-7-9-4-10	4.48
10	Standard cargo trucks	10-8-3-10	4.42

The “Optimal Ratio” column in Table 5 represents the proportion of the number of times the algorithm achieved the optimal cost to the total number of rounds.

To validate the effectiveness and generalizability of the designed algorithm, simulation construction parameters were adjusted and resolved.

Changes were made to various vehicle types:

- The payload capacity of refrigerated trucks was increased to 7 tons, and their unit transportation costs were raised to USD 6 per unit distance.
- The daily startup costs of fragile cargo trucks were reduced to USD 3 per day, and their unit transportation costs were raised to USD 5 per unit distance.
- The payload capacity of standard cargo trucks was raised to 6 tons. The unit transportation costs for standard cargo trucks were raised to USD 10 per unit distance, and the daily startup costs were reduced to USD 8 per day.

Under these revised conditions, the resultant cost data following these changes are presented in Table 7. The optimal paths and loads for each type of cargo obtained by the algorithm are shown in Table 8.

Table 7. Cost data results.

Cost	Lévy-EGACO			ACO			AGA		
	Best	Average	Optimal Ratio	Best	Average	Optimal Ratio	Best	Average	Optimal Ratio
Refrigerated	97.2	97.2	100%	99.6	101.67	10%	99.6	101.61	10%
Fragile	53.5	53.5	100%	53.5	53.5	100%	53.5	53.5	100%
Standard	106.4	106.46	95%	107.6	108.32	45%	107.6	107.99	50%
Total	257.1	257.16	-	260.7	263.49	-	260.7	263.1	-



**Table 8.** Transportation routes for each vehicle type.

Number	Vehicle Type	Transportation Route	Load/Ton
1	Refrigerated cargo trucks	10-8-7-9-5-10	6.83
2	Refrigerated cargo trucks	10-4-1-2-10	6.77
3	Refrigerated cargo trucks	10-3-6-10	1.45
4	Fragile cargo trucks	10-6-3-5-1-2-10	1.85
5	Fragile cargo trucks	10-8-7-9-4-10	1.38
6	Standard cargo trucks	10-4-1-2-10	5.68
7	Standard cargo trucks	10-8-7-9-10	5.91
8	Standard cargo trucks	10-3-5-10	4.3
9	Standard cargo trucks	10-6-10	1.76

#### 4.3. Data Analysis

From the comparative analysis presented in Tables 5 and 7, it is evident that Lévy-EGACO demonstrates enhanced stability and reliability in solving the MT-CVRP. Within 20 rounds of solution trials, Lévy-EGACO nearly reached the known optimal cost values in every attempt, whereas both the standard ACO and AGA algorithms frequently fell into local optima, preventing them from achieving the lowest average costs. Moreover, before the base data modification, Lévy-EGACO reduced the average cost by 1.8% compared to standard ACO and by 1.9% compared to AGA. After the data changes, in the second round of testing, this reduction increased to 2.5% and 2.3%, respectively.

Additionally, from the perspective of solution correctness, as observed in Tables 6 and 8, the routes for each vehicle type are very rational with no repetitions or omissions of any station. For refrigerated cargo trucks, the increase in load allowed a reduction in the number of transport vehicles needed, which decreased the overall costs despite an increase in per-kilometer transportation costs. For fragile cargo trucks, there was no change in load capacity, which meant that within the load limits, there were no additional route options available even though the daily startup and per-kilometer transportation costs were altered. For standard cargo trucks, which had all base data altered, the algorithm significantly changed the routes to effectively reduce the total costs. The load of each vehicle during individual transports did not exceed the set load limits, and the variations in simulation conditions leading to changes in the results also conformed to all constraints and theoretical expectations.

Thus, it is clear that Lévy-EGACO significantly outperforms the standard ACO algorithm in solving the MT-CVRP, demonstrating its superiority.

#### 5. Conclusions

In this investigation of the MT-CVRP, the study rigorously examines the deployment of ACO techniques, introducing the Lévy-EGACO algorithm. The efficacy of Lévy-EGACO in solving the MT-CVRP has been substantiated through comprehensive simulation trials. Importantly, the integration of elitist guidance alongside Lévy flight mechanisms enriches the pheromone update process, significantly broadening diversity and effectively circumventing the issue of premature convergence to local optima.

Looking forward, the research agenda for the algorithm could shift toward exploring a broader range of adaptive strategies to enhance both its applicability and practical effectiveness. Sensitivity analysis could be carried out to study the influence degree of each parameter on the target, which can optimize the location of distribution sites, thereby improving the utilization of vehicles and the robustness of the model under various extreme conditions. Additionally, the incorporation of parallelization strategies could further adapt the algorithm for larger-scale scenarios and real-world complex scenarios. The findings of this research endeavor to contribute valuable insights to the academic community, encouraging sustained scholarly inquiry and innovation within this domain.

**Author Contributions:** Conceptualization, L.T. and K.Z.; methodology, J.Y.; software, K.Z.; data curation, J.Y.; writing—original draft preparation, L.T.; writing—review and editing, J.Y.; supervision, L.T. All authors have read and agreed to the published version of the manuscript.

**Funding:** This research was funded by The National Natural Science Foundation of China, grant number U1636208.

**Data Availability Statement:** The data presented in this study are available in this article.

**Conflicts of Interest:** The authors declare no conflicts of interest.

## References

1. Sarbijan, M.S.; Behnamian, J. Emerging Research Fields in Vehicle Routing Problem: A Short Review. *Arch. Comput. Method Eng.* **2023**, *30*, 2473–2491. [[CrossRef](#)]
2. Elshaer, R.; Awad, H. A Taxonomic Review of Metaheuristic Algorithms for Solving the Vehicle Routing Problem and Its Variants. *Comput. Ind. Eng.* **2020**, *140*, 106242. [[CrossRef](#)]
3. Ni, Q.; Tang, Y. A Bibliometric Visualized Analysis and Classification of Vehicle Routing Problem Research. *Sustainability* **2023**, *15*, 7394. [[CrossRef](#)]
4. Sarbijan, M.S.; Behnamian, J. Multi-Fleet Feeder Vehicle Routing Problem Using Hybrid Metaheuristic. *Comput. Oper. Res.* **2022**, *141*, 105696. [[CrossRef](#)]
5. Alssager, M.; Othman, Z.A.; Ayob, M.; Mohamad, R.; Yuliansyah, H. Hybrid Cuckoo Search for the Capacitated Vehicle Routing Problem. *Symmetry* **2020**, *12*, 2088. [[CrossRef](#)]
6. Holló-Szabó, Á.; Botzheim, J. Bacterial Memetic Algorithm for Asymmetric Capacitated Vehicle-Routing Problem. *Electronics* **2022**, *11*, 3758. [[CrossRef](#)]
7. Yang, F.; Tao, F. A Bi-Objective Optimization VRP Model for Cold Chain Logistics: Enhancing Cost Efficiency and Customer Satisfaction. *IEEE Access* **2023**, *11*, 127043–127056. [[CrossRef](#)]
8. Gu, Z.; Zhu, Y.; Wang, Y.; Du, X.; Guizani, M.; Tian, Z. Applying Artificial Bee Colony Algorithm to the Multidepot Vehicle Routing Problem. *Softw.-Pract. Exp.* **2022**, *52*, 756–771. [[CrossRef](#)]
9. Ahmed, Z.H.; Hameed, A.S.; Mutar, M.L. Hybrid Genetic Algorithms for the Asymmetric Distance-Constrained Vehicle Routing Problem. *Math. Probl. Eng.* **2022**, *2022*, 2435002. [[CrossRef](#)]
10. Li, C.; Zhu, Y.; Lee, K.Y. Route Optimization of Electric Vehicles Based on Reinsertion Genetic Algorithm. *IEEE Trans. Transp. Electr.* **2023**, *9*, 3753–3768. [[CrossRef](#)]
11. Liu, D.; Deng, Z.; Mao, X.; Yang, Y.; Kaisar, E.I. Two-Echelon Vehicle-Routing Problem: Optimization of Autonomous Delivery Vehicle-Assisted E-Grocery Distribution. *IEEE Access* **2020**, *8*, 108705–108719. [[CrossRef](#)]
12. Ji, X.-F.; Pan, J.-S.; Chu, S.-C.; Hu, P.; Chai, Q.-W.; Zhang, P. Adaptive Cat Swarm Optimization Algorithm and Its Applications in Vehicle Routing Problems. *Math. Probl. Eng.* **2020**, *2020*, 1291526. [[CrossRef](#)]
13. Zacharia, P.; Drosos, C.; Piromalis, D.; Papoutsidakis, M. The Vehicle Routing Problem with Fuzzy Payloads Considering Fuel Consumption. *Appl. Artif. Intell.* **2021**, *35*, 1755–1776. [[CrossRef](#)]
14. Leng, K.; Li, S. Distribution Path Optimization for Intelligent Logistics Vehicles of Urban Rail Transportation Using VRP Optimization Model. *IEEE Trans. Intell. Transp. Syst.* **2022**, *23*, 1661–1669. [[CrossRef](#)]
15. Dorigo, M.; Blum, C. Ant Colony Optimization Theory: A Survey. *Theor. Comput. Sci.* **2005**, *344*, 243–278. [[CrossRef](#)]
16. Almufti, S.; Maribojoc, R.; Pahiriray, A. Ant Based System: Overview, Modifications and Applications from 1992 to 2022. *Polaris Glob. J. Sch. Res. Trends* **2022**, *1*, 29–37. [[CrossRef](#)]
17. Liu, M.; Song, Q.; Zhao, Q.; Li, L.; Yang, Z.; Zhang, Y. A Hybrid BSO-ACO for Dynamic Vehicle Routing Problem on Real-World Road Networks. *IEEE Access* **2022**, *10*, 118302–118312. [[CrossRef](#)]
18. Yin, C.; Fang, Q.; Li, H.; Peng, Y.; Xu, X.; Tang, D. An Optimized Resource Scheduling Algorithm Based on GA and ACO Algorithm in Fog Computing. *J. Supercomput.* **2024**, *80*, 4248–4285. [[CrossRef](#)]
19. Duraiswamy, A.; Selvam, G. An Ant Colony-Based Optimization Model for Resource-Leveling Problem. In *Proceedings of the Advances in Construction Management, Acmm 2021*; Loon, L.Y., Subramanian, M., Gunasekaran, K., Eds.; Springer-Verlag Singapore Pte Ltd.: Singapore, 2022; Volume 191, pp. 333–342.
20. Maheshwari, P.; Sharma, A.K.; Verma, K. Energy Efficient Cluster Based Routing Protocol for WSN Using Butterfly Optimization Algorithm and Ant Colony Optimization. *Ad Hoc Netw.* **2021**, *110*, 102317. [[CrossRef](#)]
21. Lesch, V.; König, M.; Kounev, S.; Stein, A.; Krupitzer, C. Tackling the Rich Vehicle Routing Problem with Nature-Inspired Algorithms. *Appl. Intell.* **2022**, *52*, 9476–9500. [[CrossRef](#)]
22. Huang, S.-H.; Huang, Y.-H.; Blazquez, C.A.; Chen, C.-Y. Solving the Vehicle Routing Problem with Drone for Delivery Services Using an Ant Colony Optimization Algorithm. *Adv. Eng. Inform.* **2022**, *51*, 101536. [[CrossRef](#)]
23. Frias, N.; Johnson, F.; Valle, C. Hybrid Algorithms for Energy Minimizing Vehicle Routing Problem: Integrating Clusterization and Ant Colony Optimization. *IEEE Access* **2023**, *11*, 125800–125821. [[CrossRef](#)]
24. Dorigo, M.; Stützle, T. Ant Colony Optimization: Overview and Recent Advances. In *Handbook of Metaheuristics*; Gendreau, M., Potvin, J.-Y., Eds.; Springer International Publishing: Cham, Switzerland, 2019; pp. 311–351. ISBN 978-3-319-91086-4.

25. Li, J.; An, Q.; Lei, H.; Deng, Q.; Wang, G.-G. Survey of Levy Flight-Based Metaheuristics for Optimization. *Mathematics* **2022**, *10*, 2785. [[CrossRef](#)]
26. Shen, Y.; Peng, L.; Li, J. An Improved Estimation of Distribution Algorithm for Multi-Compartment Electric Vehicle Routing Problem. *J. Syst. Eng. Electron.* **2021**, *32*, 365–379. [[CrossRef](#)]
27. Odili, J.B.; Noraziah, A.; Zarina, M. A Comparative Performance Analysis of Computational Intelligence Techniques to Solve the Asymmetric Travelling Salesman Problem. *Comput. Intell. Neurosci.* **2021**, *2021*, 6625438. [[CrossRef](#)]

**Disclaimer/Publisher's Note:** The statements, opinions and data contained in all publications are solely those of the individual author(s) and contributor(s) and not of MDPI and/or the editor(s). MDPI and/or the editor(s) disclaim responsibility for any injury to people or property resulting from any ideas, methods, instructions or products referred to in the content.